

Supplemental material

For the article "Cascading effects augment the direct impact of CO₂ on phytoplankton growth in a biogeochemical model"

Miriam Seifert^{1,*}, Cara Nissen¹, Björn Rost^{1,2}, and Judith Hauck¹

¹ Alfred-Wegener-Institut Helmholtz-Zentrum für Polar- und Meeresforschung, Am Handelshafen 12, 27570 Bremerhaven, Germany

² Universität Bremen, FB2, Leobener Straße, 28359 Bremen, Germany

* miriam.seifert@awi.de

Content:

Text S1: Analysis of coccolithophore niche occupation

Figure S1: Temperature sensitivities f^T of coccolithophores, diatoms, and small phytoplankton

Figure S2: Function fits for growth rates of coccolithophores, diatoms, and small phytoplankton, as well as (PIC:POC)_{cocco} ratios

Figure S3: Sensitivity of phytoplankton biomass towards the parameter choice of CO₂ dependencies

Figure S4: Hovmöller plots of the mixed-layer mean coccolithophore biomass concentration

Figure S5: Depth distribution on the upper 200 m of coccolithophore, diatom, and small-phytoplankton biomass

Figure S6: Relative changes in surface chlorophyll-to-carbon ratios as well as chlorophyll and carbon concentrations

Table S1: Reference included into the function fits for growth and calcification dependence

References

Text S1: Analysis of coccolithophore niche occupation

To investigate whether the simulated coccolithophore distribution captures different ecological niches of coccolithophores observed in the ocean (e.g., Brun et al., 2015; O'Brien et al., 2016), we compared the model results of the PRESENT_CO2 and the PRESENT simulations to a gridded product of global coccolithophore biomass that is based on a statistical feed-forward neural network methodology and reveals the distribution of coccolithophore clusters in the MAREDAT dataset (O'Brien, 2015). The niche analysis of O'Brien (2015) yields mixed-layer averaged biomass of three coccolithophore clusters, namely a warm water cluster comprising 19 species, a cold water cluster comprising three species, and a cluster consisting only of *E. huxleyi*, that are separated by their preferred PAR, nitrate, silicate, excess phosphate, temperature, and mixed layer depth ranges. Both in the mixed layer product used by O'Brien (2015) and in our model, the mixed layer depth is defined by a density criterion of 0.03 kg m^{-3} (de Boyer Montégut et al., 2004). Our model output yields 20–30 m deeper mixed layer depths in the tropics and subtropics than the product used by O'Brien (2015), and similarly deep mixed layer depths further north/south during the respective growing season at each hemisphere, except from parts of the Southern Ocean where the gridded product of O'Brien (2015) displays a deeper summer mixed layer (not shown). We computed the correlation of either zonally or monthly averaged coccolithophore biomass concentrations in the statistical model for the three clusters and our modelled coccolithophore biomass. Due to possible spatial or temporal mismatches between the statistical model and our model which can both be subject to biases (for the statistical model discussed in O'Brien, 2015), we chose the Spearman correlation instead of the commonly used Pearson correlation, as it assesses the monotonic relationship between two datasets and therefore omits mismatches in space, time, and magnitude. For the comparison between our model and the statistical model, we are more interested in general patterns and less in perfect spatial and temporal fits and total magnitudes of coccolithophore biomass.

Spearman correlations are similar in the PRESENT and the PRESENT_CO2 simulation, and we focus here on the comparison of the PRESENT simulation with the statistical model of O'Brien (2015). Zonally and monthly averaged coccolithophore biomass concentrations in the mixed layer are higher in our model compared to the statistical model, especially in the northern hemisphere and the equatorial region (Figure S4). This coincides with the comparison to the MAREDAT dataset as shown in Section *Representation of coccolithophores and biogeochemical fluxes in FESOM-REcoM* and Figure 3A. Additionally, we attribute locally higher biomass concentrations to a deeper mixed layer depth of our model compared to that of O'Brien (2015), especially in the tropical and subtropical regions, and a coccolithophore distribution over a wide depth range (Figure S5), likely capturing a larger share of total coccolithophore biomass than O'Brien (2015). The comparison between our model and the sum of all clusters yields a Spearman correlation coefficient of 0.60 for the entire model grid. The Spearman correlations with the three clusters separately (*E. huxleyi*, warm, cold) are 0.62, 0.55, and –0.02,

respectively, indicating that the bloom-forming *E. huxleyi* and the warm cluster are equally well represented by our model, while the cold cluster is not represented. This is possibly because we excluded coccolithophore growth in regions with temperatures $<0^{\circ}\text{C}$ (Equation 3) and, thus, suppress coccolithophore occurrence in most parts of the Arctic and the Southern Ocean during winter. Fast bloom formation might thereby be impeded at temperatures $>0^{\circ}\text{C}$ in spring, and therefore a poor correlation with the cold cluster was to be expected. The Spearman correlation of our model with the sum of the *E. huxleyi* and the warm cluster is 0.66. The fact that the warm cluster is as well represented in our model as the *E. huxleyi* cluster makes us confident that our model displays a broad variety of coccolithophore species, despite the bias towards *E. huxleyi* in our selection of laboratory studies. To investigate the correlations with our model along both the spatial and temporal axes, we calculated zonally averaged monthly coefficients and monthly averaged zonal coefficients for the summed *E. huxleyi* and warm cluster (small panels in Figure S4F). Monthly Spearman correlations reveal that the coefficient is lowest between January and April (<0.5). We attribute this to a longer bloom duration at $40\text{--}50^{\circ}\text{S}$ in our model compared to the statistical model, as well as a spring bloom at $10\text{--}20^{\circ}\text{N}$ that is not visible in the statistical model (Figure S4A). Latitudinal Spearman correlation is low where blooms in the model are shifted towards lower latitudes compared to the statistical model, for example at 10°N and $50\text{--}60^{\circ}\text{S}$ (Figure S4F).

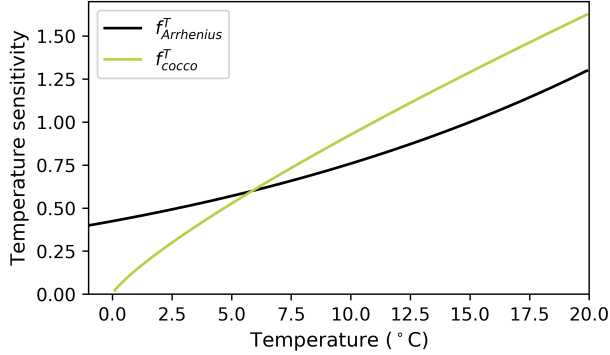


Figure S1: Temperature sensitivities f^T of coccolithophores, diatoms, and small phytoplankton. The coccolithophore temperature sensitivity (f_{cocco}^T) follows Fielding (2013) and the diatom and small-phytoplankton temperature sensitivity ($f_{Arrhenius}^T$) follows Equations 3 and 4.

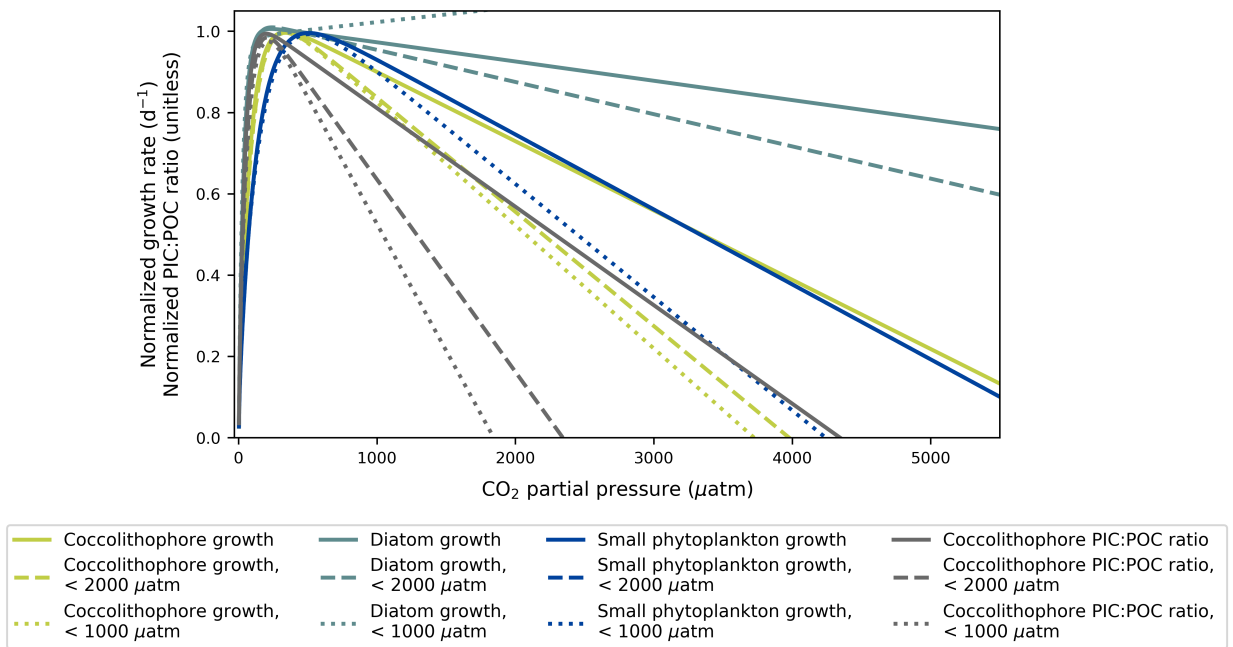


Figure S2: Function fits for growth rates of coccolithophores, diatoms, and small phytoplankton, as well as (PIC:POC)_{cocco} ratios. The graph indicates fits for the entire pCO₂ range as shown in Figure 1, as well as fits to subsets of laboratory measurements with < 2000 μatm and < 1000 μatm pCO₂. Note that all laboratory data points for small-phytoplankton growth are < 2000 μatm and, hence, the fit for the entire pCO₂ range is similar to the fit for the range < 2000 μatm pCO₂. Because of the limited constraints of the diatom function fit for datapoints < 1000 μatm pCO₂, the shape of the curve is distorted.

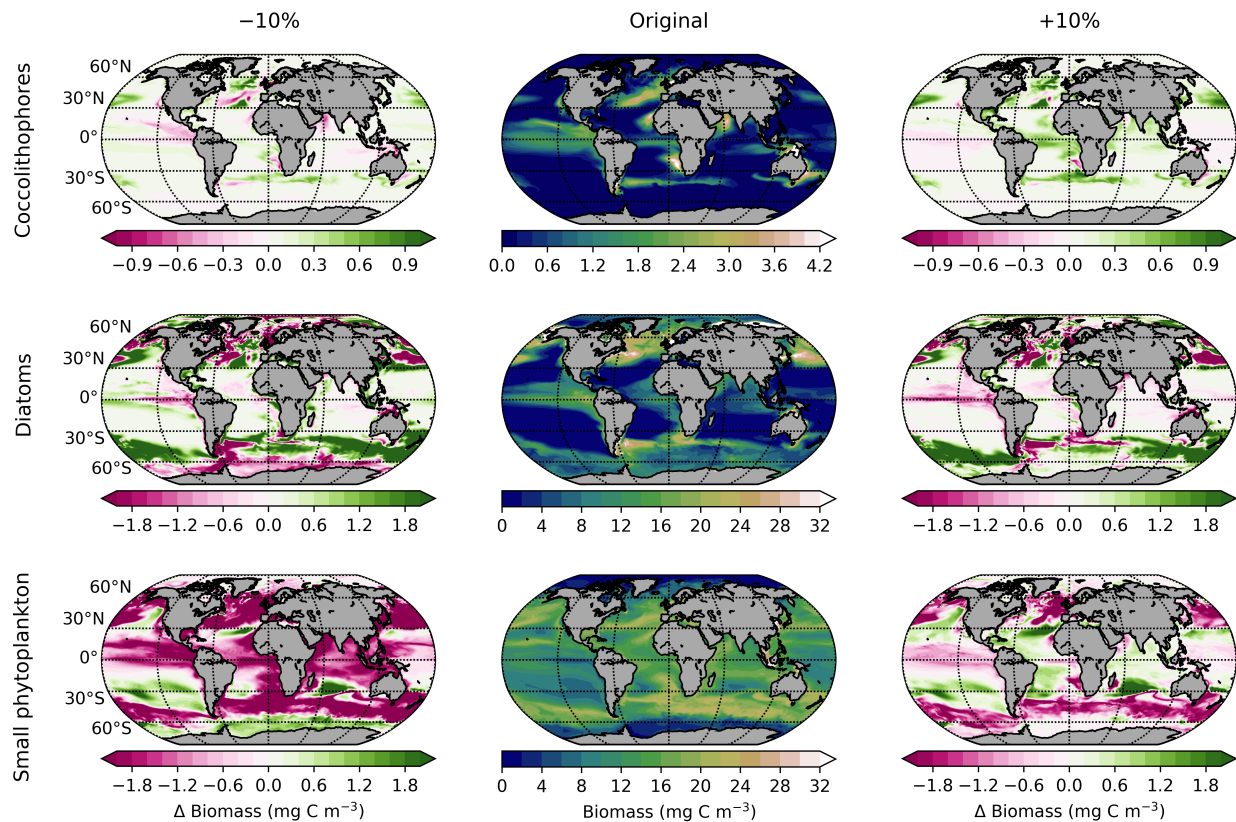


Figure S3: Sensitivity of phytoplankton biomass towards the parameter choice of CO_2 dependencies. Mean phytoplankton biomass concentrations over the upper 150 m of the watercolumn in the PRESENT_CO2 simulation (middle column), and difference to simulations in which the parameters a, b, c, and d were modified by -10% (left column) and +10% (right column), respectively. Note the different colorscales of coccolithophores compared to diatoms and small phytoplankton.

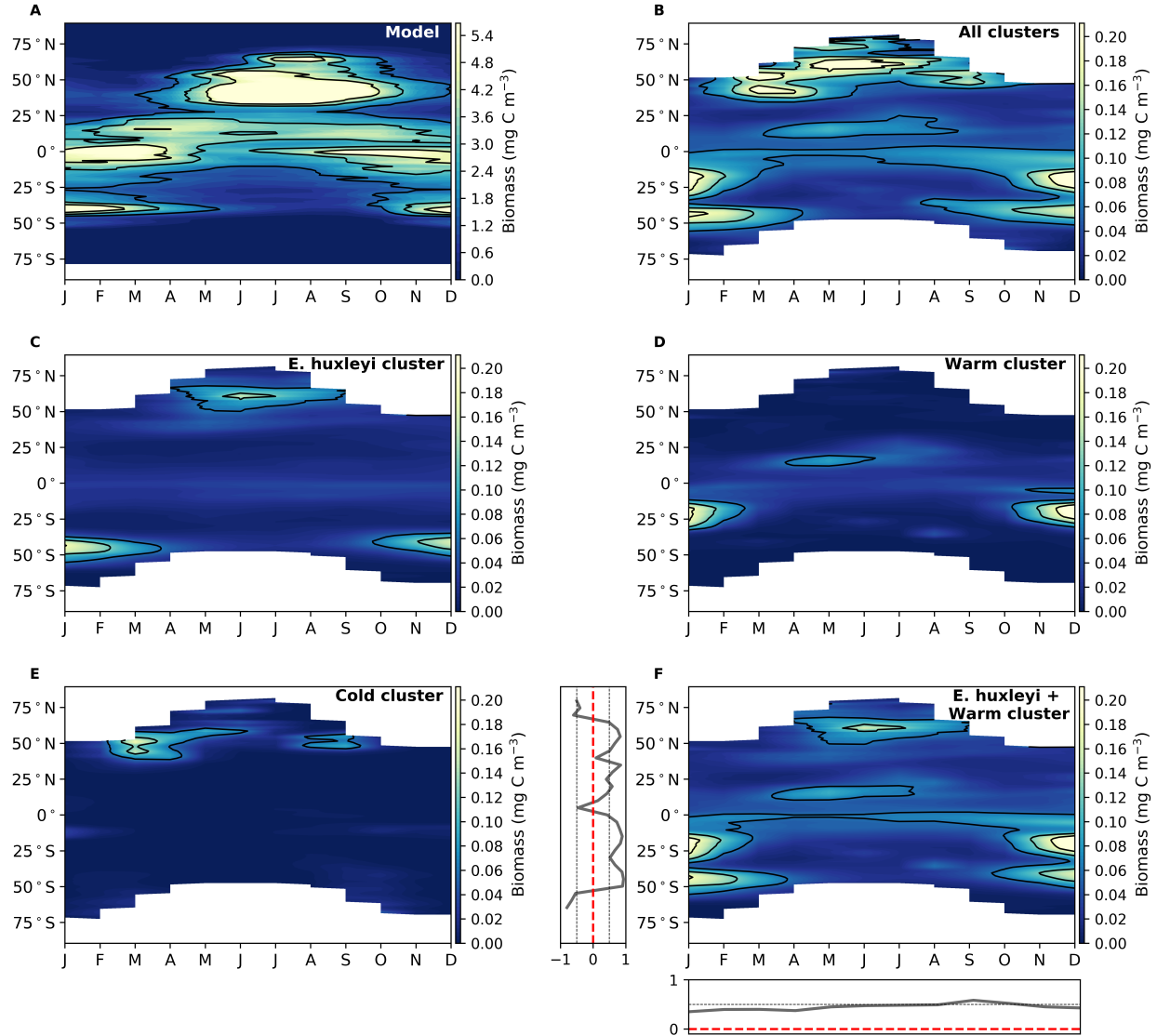


Figure S4: Hovmöller plots of the mixed-layer mean coccolithophore biomass concentration Panels (after Hovmöller, 1949) display (A) the PRESENT simulation (isolines in steps of 1.5 mg C m^{-3}), and (B–F) the statistical model of O'Brien (2015) (isolines in steps of 0.06 mg C m^{-3}). Panel B depicts the sum of the cold, warm and *E. huxleyi* cluster. Line plots at the left and bottom side of panel F visualize Spearman correlations that were computed for each month over the entire latitudinal distribution, and for 5° latitudinal bins over all months (for bins with data of minimum three months). White areas in the plots of the statistical model display regions with scarce data coverage that were omitted from data interpolation.

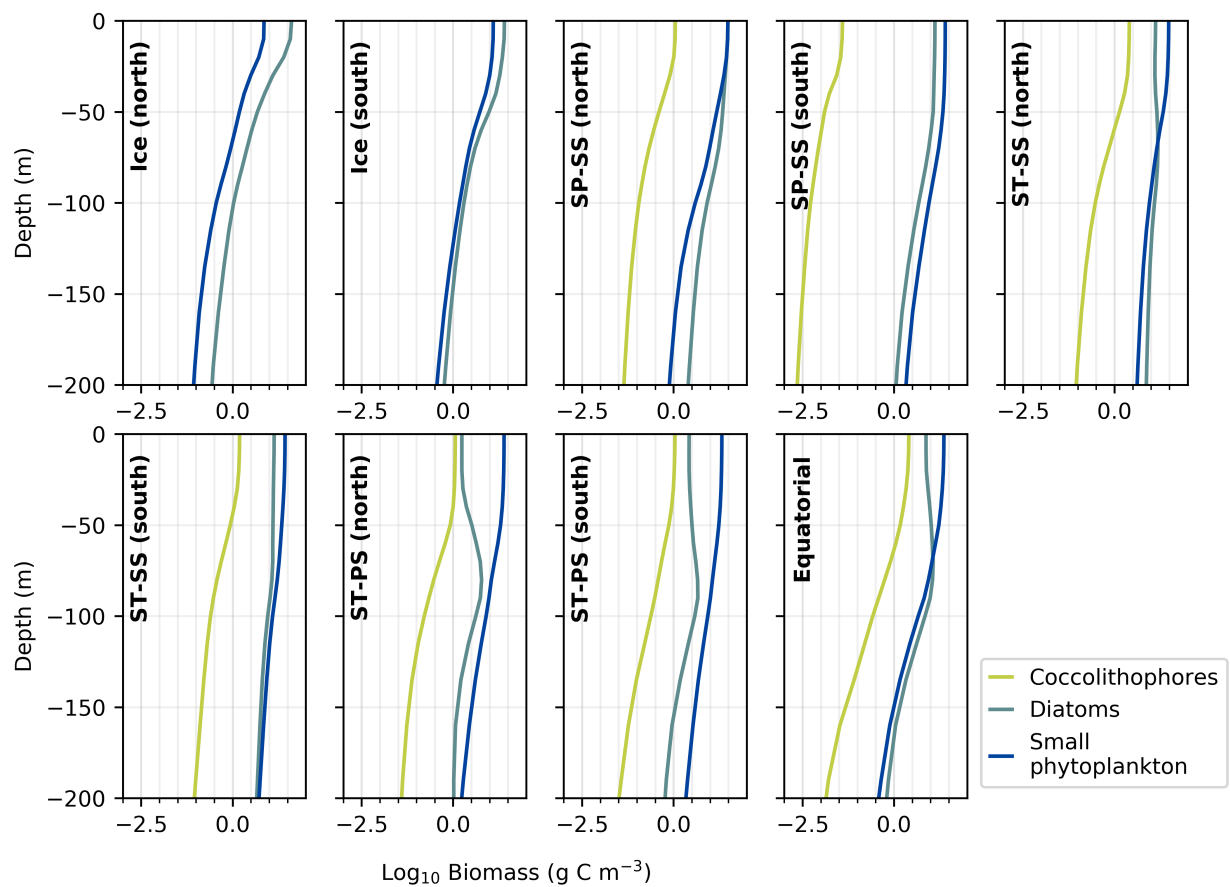


Figure S5: Depth distribution in the upper 200 m of coccolithophore, diatom, and small-phytoplankton biomass. Panels display mean biomass concentrations at each depth level in oceanic biomes after Fay and McKinley (2014), displayed in logarithmic scale. Note that coccolithophores were omitted in ice regions because of their low biomasses. SP = subpolar, ST = subtropic, SS = seasonal stratified, PS = permanent stratified.

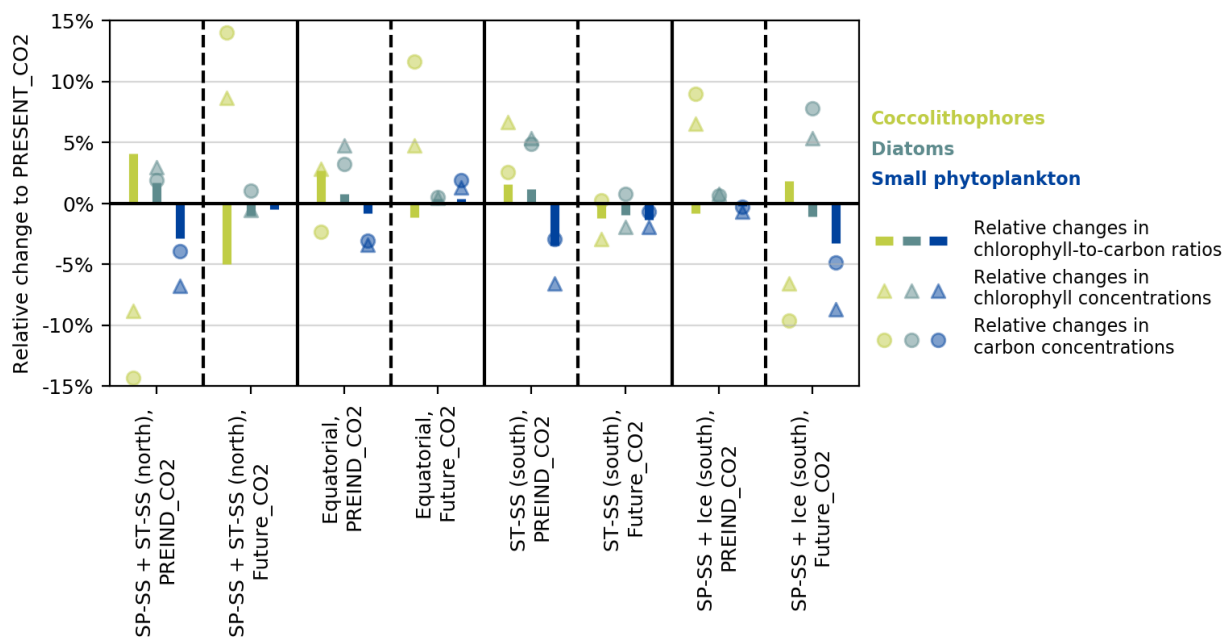


Figure S6: Relative changes in surface chlorophyll-to-carbon ratios as well as chlorophyll and carbon concentrations. Values are compared between the PRESENT_CO2 and the FUTURE_CO2 (right) simulation in all focus regions introduced in Figure 7.

Table S1: (Part I) Reference included into the function fits for growth and calcification dependence.

Reference	Species	Region	Temp. (°C)	$p\text{CO}_{2\text{opt}}$ (μatm)	# CO_2 levels
Coccolithophores					
Bach et al. (2011)	<i>Emiliana huxleyi</i>	?	15	198, 248, 440	>10
Bach et al. (2015)	<i>Coccolithus pelagicus</i>	?	15	187, 251, 498	>10
Feng et al. (2017)	<i>Emiliana huxleyi</i>	New Zealand	14	180	6
Hermoso (2015)	<i>Coccolithus pelagicus</i>	?	15	514	7
Hermoso (2015)	<i>Gephyrocapsa oceanica</i>	?	15	166	9
Hoppe et al. (2011)	<i>Emiliana huxleyi</i>	Iceland	15	223	4
Hoppe et al. (2011)	<i>Emiliana huxleyi</i>	Iceland	15	440	4
Hoppe et al. (2011)	<i>Emiliana huxleyi</i>	New Zealand	15	148	4
Hoppe et al. (2011)	<i>Emiliana huxleyi</i>	New Zealand	15	276	4
Hoppe et al. (2011)	<i>Emiliana huxleyi</i>	New Zealand	15	577	4
Kottmeier et al. (2016)	<i>Emiliana huxleyi</i>	?	15	356, 595, 1242	3
Krug et al. (2011)	<i>Coccolithus braarudii</i>	South Atlantic	17	484	>10
Krug et al. (2011)	<i>Coccolithus braarudii</i>	South Atlantic	17	1117, 1221, 1253	>10
Langer et al. (2006)	<i>Calcidiscus leptoporus</i>	South Atlantic	20	216, 345	6
Langer et al. (2006)	<i>Calcidiscus leptoporus</i>	South Atlantic	17	149	3
Langer et al. (2009)	<i>Emiliana huxley</i>	North Pacific	20	675	4
Langer et al. (2009)	<i>Emiliana huxley</i>	Tasmanian Sea	17	217, 420	4
Langer et al. (2009)	<i>Emiliana huxley</i>	North Atlantic	17	192, 397	4
Langer et al. (2009)	<i>Emiliana huxley</i>	South Atlantic	20	193	4
Müller et al. (2015)	<i>Emiliana huxley</i>	Tasmanian Sea	14	386	6
Müller et al. (2015)	<i>Emiliana huxley</i>	Southern Ocean	14	277, 389	6
Müller et al. (2015)	<i>Emiliana huxley</i>	Southern Ocean	14	626	6
Riebesell et al. (2000)	<i>Emiliana huxleyi</i>	?	15	302	5
Sett et al. (2014)	<i>Gephyrocapsa oceanica</i>	Arcachon Bay	15	262	>10
Sett et al. (2014)	<i>Gephyrocapsa oceanica</i>	Arcachon Bay	20	377	>10
Sett et al. (2014)	<i>Gephyrocapsa oceanica</i>	Arcachon Bay	25	342	>10
Sett et al. (2014)	<i>Gephyrocapsa oceanica</i>	Bergen	10	465	>10
Sett et al. (2014)	<i>Gephyrocapsa oceanica</i>	Bergen	15	193, 265, 453	>10
Sett et al. (2014)	<i>Gephyrocapsa oceanica</i>	Bergen	20	1224	>10

Table S2: (Part II) Reference included into the function fits for growth and calcification dependence.

Reference	Species	Region	Temp. (°C)	$p\text{CO}_{2\text{opt}}$ (μatm)	# CO_2 levels
Diatoms					
Barcelos e Ramos et al. (2014)	<i>Asterionellopsis glacialis</i>	Azores	20	331, 817	>10
Ihnken et al. (2011)	<i>Chaetoceros muelleri</i>	Tasman Sea	22	643	3
Ihnken et al. (2011)	<i>Chaetoceros muelleri</i>	Tasman Sea	22	1624	3
Ihnken et al. (2011)	<i>Chaetoceros muelleri</i>	Tasman Sea	22	643	3
Ihnken et al. (2011)	<i>Chaetoceros muelleri</i>	Tasman Sea	22	643	3
Li et al. (2019)	<i>Thalassiosira weissflogii</i>	Daya Bay, China	10	390	>10
Pančić et al. (2015)	<i>Fragilariopsis cylindrus</i>	Greenland	1	631	4
Pančić et al. (2015)	<i>Fragilariopsis cylindrus</i>	Greenland	5	1226	8
Pančić et al. (2015)	<i>Fragilariopsis cylindrus</i>	Greenland	8	584	9
Pančić et al. (2015)	<i>Fragilariopsis cylindrus</i>	Greenland	1	648	7
Pančić et al. (2015)	<i>Fragilariopsis cylindrus</i>	Greenland	5	2652	9
Pančić et al. (2015)	<i>Fragilariopsis cylindrus</i>	Greenland	10	677	10
Pančić et al. (2015)	<i>Fragilariopsis cylindrus</i>	Greenland	1	2309	8
Pančić et al. (2015)	<i>Fragilariopsis cylindrus</i>	Greenland	5	1995	9
Pančić et al. (2015)	<i>Fragilariopsis cylindrus</i>	Greenland	8	1990	6
Pančić et al. (2015)	<i>Fragilariopsis cylindrus</i>	Greenland	5	2486	7
Pančić et al. (2015)	<i>Fragilariopsis cylindrus</i>	Greenland	5	601	7
Pančić et al. (2015)	<i>Fragilariopsis cylindrus</i>	Greenland	5	2655	7
Pančić et al. (2015)	<i>Fragilariopsis cylindrus</i>	Greenland	1	633	7
Pančić et al. (2015)	<i>Fragilariopsis cylindrus</i>	Greenland	5	1231	8
Pančić et al. (2015)	<i>Fragilariopsis cylindrus</i>	Greenland	8	586	6
Sugie and Yoshimura (2013)	<i>Pseudo-nitzschia pseudodelicatissima</i>	Seto Island Sea, Japan	20	339, 475	8
Sugie and Yoshimura (2013)	<i>Pseudo-nitzschia pseudodelicatissima</i>	Seto Island Sea, Japan	20	160	8
Sugie and Yoshimura (2016)	<i>Thalassiosira weissflogii</i>	?	20	628	6
Tatters et al. (2013)	<i>Cylindotheca fusiformis</i>	New Zealand	14	152	3
Tatters et al. (2013)	<i>Cosinodiscus sp.</i>	New Zealand	14	428	3
Tatters et al. (2013)	<i>Thalassiosira sp.</i>	New Zealand	14	297	3

Table S3: (Part III) Reference included into the function fits for growth and calcification dependence.

Reference	Species	Region	Temp. (°C)	pCO ₂ _{opt} (μatm)	# CO ₂ levels
Diatoms					
Tatters et al. (2013)	<i>Pseudonitzschia delicatissima</i>	New Zealand	14	152	3
Tatters et al. (2013)	<i>Navicula sp.</i>	New Zealand	14	152	3
Tatters et al. (2013)	<i>Chaetoceros criophilus</i>	New Zealand	14	428	3
Tatters et al. (2013)	<i>Cylindotheca fusiformis</i>	New Zealand	19	184	3
Tatters et al. (2013)	<i>Cosinodiscus sp.</i>	New Zealand	19	450	3
Tatters et al. (2013)	<i>Thalassiosira sp.</i>	New Zealand	19	450	3
Tatters et al. (2013)	<i>Pseudonitzschia delicatissima</i>	New Zealand	19	184	3
Tatters et al. (2013)	<i>Navicula sp.</i>	New Zealand	19	450	3
Tatters et al. (2013)	<i>Chaetoceros criophilus</i>	New Zealand	19	450	3
Tatters et al. (2013)	<i>Cylindotheca fusiformis</i>	New Zealand	14	122	3
Tatters et al. (2013)	<i>Cosinodiscus sp.</i>	New Zealand	14	222	3
Tatters et al. (2013)	<i>Thalassiosira sp.</i>	New Zealand	14	122	3
Tatters et al. (2013)	<i>Pseudonitzschia delicatissima</i>	New Zealand	14	122	3
Tatters et al. (2013)	<i>Navicula sp.</i>	New Zealand	14	122, 222, 328	3
Tatters et al. (2013)	<i>Chaetoceros criophilus</i>	New Zealand	14	122	3
Tatters et al. (2013)	<i>Cylindotheca fusiformis</i>	New Zealand	19	152	3
Tatters et al. (2013)	<i>Cosinodiscus sp.</i>	New Zealand	19	152, 428	3
Tatters et al. (2013)	<i>Thalassiosira sp.</i>	New Zealand	19	253	3
Tatters et al. (2013)	<i>Pseudonitzschia delicatissima</i>	New Zealand	19	253	3
Tatters et al. (2013)	<i>Navicula sp.</i>	New Zealand	19	428	3
Tatters et al. (2013)	<i>Chaetoceros criophilus</i>	New Zealand	19	152, 428	3
Trimborn et al. (2013)	<i>Chaetoceros debilis</i>	Southern Ocean	3	982	3
Trimborn et al. (2013)	<i>Pseudo-nitzschia subcurvata</i>	Southern Ocean	3	401	3
Trimborn et al. (2013)	<i>Phaeocystis antarctica</i>	Southern Ocean	3	162	3
Wolf et al. (2018)	<i>Thalassiosira hyalina</i>	Kongsfjorden	3	388	4
Wolf et al. (2018)	<i>Thalassiosira hyalina</i>	Kongsfjorden	6	348	4
Wolf et al. (2018)	<i>Thalassiosira hyalina</i>	Kongsfjorden	3	687	4
Wolf et al. (2018)	<i>Thalassiosira hyalina</i>	Kongsfjorden	6	1362	4

Table S4: (Part IV) Reference included into the function fits for growth and calcification dependence.

Reference	Species	Region	Temp. (°C)	pCO _{2opt} (μatm)	# CO ₂ levels
Small phytoplankton					
Eichner et al. (2014)	<i>Trichodesmium erythraeum</i>	?	25	175	3
Eichner et al. (2014)	<i>Trichodesmium erythraeum</i>	?	25	363	3
Garcia et al. (2013)	<i>Crocospaera watsonii</i>	Equatorial Atlantic	28	387	3
Hennon et al. (2014)	<i>Heterosigma akashiwo</i>	?	18	693	>10
Hoppe et al. (2018)	<i>Micromonas pusilla</i>	Kongsfjorden	2	335, 1322	>10
Hoppe et al. (2018)	<i>Micromonas pusilla</i>	Kongsfjorden	6	1030, 1069	>10
Kim et al. (2013)	<i>Heterosigma akashiwo</i>	Rhode Island	15	1148	3
Kranz et al. (2009)	<i>Trichodesmium erythraeum</i>	?	25	119, 291, 745	3
(PIC:POC)_{cocco} ratio					
Bach et al. (2011)	<i>Emiliania huxleyi</i>	?	15	375	>10
Bach et al. (2015)	<i>Coccolithus pelagicus</i>	?	15	251	>10
Feng et al. (2017)	<i>Emiliania huxleyi</i>	New Zealand	14	102	6
Hoppe et al. (2011)	<i>Emiliania huxleyi</i>	Iceland	15	215	4
Hoppe et al. (2011)	<i>Emiliania huxleyi</i>	Iceland	15	148	4
Hoppe et al. (2011)	<i>Emiliania huxleyi</i>	New Zealand	15	265	4
Hoppe et al. (2011)	<i>Emiliania huxleyi</i>	New Zealand	15	159	4
Hoppe et al. (2011)	<i>Emiliania huxleyi</i>	New Zealand	15	281	4
Krug et al. (2011)	<i>Coccolithus braarudii</i>	South Atlantic	17	1257	>10
Krug et al. (2011)	<i>Coccolithus braarudii</i>	South Atlantic	17	388, 879	>10
Langer et al. (2006)	<i>Calcidiscus leptopus</i>	South Atlantic	20	345	6
Langer et al. (2006)	<i>Calcidiscus leptopus</i>	South Atlantic	17	345	3
Langer et al. (2009)	<i>Emiliania huxleyi</i>	North Pacific	20	926	4
Langer et al. (2009)	<i>Emiliania huxleyi</i>	Tasmanian Sea	17	217	4
Langer et al. (2009)	<i>Emiliania huxleyi</i>	North Atlantic	17	396	4
Langer et al. (2009)	<i>Emiliania huxleyi</i>	South Atlantic	20	193	4
Müller et al. (2015)	<i>Emiliania huxleyi</i>	Tasmanian Sea	14	386	6
Müller et al. (2015)	<i>Emiliania huxleyi</i>	Southern Ocean	14	389	6
Müller et al. (2015)	<i>Emiliania huxleyi</i>	Southern Ocean	14	626	6
Riebesell et al. (2000)	<i>Emiliania huxleyi</i>	?	15	139	5
Sett et al. (2014)	<i>Gephyrocapsa oceanica</i>	Arcachon Bay	15	54	>10
Sett et al. (2014)	<i>Gephyrocapsa oceanica</i>	Arcachon Bay	20	54	>10
Sett et al. (2014)	<i>Gephyrocapsa oceanica</i>	Bergen	10	127	>10
Sett et al. (2014)	<i>Gephyrocapsa oceanica</i>	Bergen	15	368	>10
Sett et al. (2014)	<i>Gephyrocapsa oceanica</i>	Bergen	20	81	>10

References

- Bach LT, Riebesell U, Gutowska MA, Federwisch L, Schulz KG. 2015. A unifying concept of coccolithophore sensitivity to changing carbonate chemistry embedded in an ecological framework. *Progress in Oceanography* **135**: 125–138. doi:10.1016/j.pocean.2015.04.012.
- Bach LT, Riebesell U, Schulz KG. 2011. Distinguishing between the effects of ocean acidification and ocean carbonation in the coccolithophore *Emiliania huxleyi*. *Limnology and Oceanography* **56**(6): 2040–2050. doi: 10.4319/lo.2011.56.6.2040.
- Barcelos e Ramos J, Schulz KG, Brownlee C, Sett S, Azevedo EB. 2014. Effects of increasing seawater carbon dioxide concentrations on chain formation of the diatom *Asterionellopsis glacialis*. *PLOS ONE* **9**(3): 1–8. doi:10.1371/journal.pone.0090749.
- Brun P, Vogt M, Payne MR, Gruber N, O'Brien CJ, Buitenhuis ET, Le Quéré C, Leblanc K, Luo YW. 2015. Ecological niches of open ocean phytoplankton taxa. *Limnology and Oceanography* **60**(3): 1020–1038. doi: 10.1002/lno.10074.
- de Boyer Montégut C, Madec G, Fischer AS, Lazar A, Iudicone D. 2004. Mixed layer depth over the global ocean: An examination of profile data and a profile-based climatology. *Journal of Geophysical Research: Oceans* **109**(C12). doi:<https://doi.org/10.1029/2004JC002378>.
- Eichner M, Kranz SA, Rost B. 2014. Combined effects of different CO₂ levels and N sources on the diazotrophic cyanobacterium *Trichodesmium*. *Physiologia Plantarum* **152**(2): 316–330. doi:<https://doi.org/10.1111/ppl.12172>.
- Fay AR, McKinley GA. 2014. Global open-ocean biomes: mean and temporal variability. *Earth System Science Data* **6**(2): 273–284. doi:10.5194/essd-6-273-2014.
- Feng Y, Roleda MY, Armstrong E, Boyd PW, Hurd CL. 2017. Environmental controls on the growth, photosynthetic and calcification rates of a Southern Hemisphere strain of the coccolithophore *Emiliania huxleyi*. *Limnology and Oceanography* **62**(2): 519–540. doi:10.1002/lno.10442.
- Fielding SR. 2013. *Emiliania huxleyi* specific growth rate dependence on temperature. *Limnology and Oceanography* **58**(2): 663–666. doi:10.4319/lo.2013.58.2.0663.
- Garcia NS, Fu FX, Breene CL, Yu EK, Bernhardt PW, Mulholland MR, Hutchins DA. 2013. Combined effects of CO₂ and light on large and small isolates of the unicellular N₂-fixing cyanobacterium *Crocospaera watsonii* from the western tropical Atlantic Ocean. *European Journal of Phycology* **48**(1): 128–139. doi:10.1080/09670262.2013.773383.

- Hennon GMM, Quay P, Morales RL, Swanson LM, Virginia Armbrust E. 2014. Acclimation conditions modify physiological response of the diatom *Thalassiosira pseudonana* to elevated CO₂ concentrations in a nitrate-limited chemostat. *Journal of Phycology* **50**(2): 243–253. doi:10.1111/jpy.12156.
- Hermoso M. 2015. Control of ambient pH on growth and stable isotopes in phytoplanktonic calcifying algae. *Paleoceanography* **30**(8): 1100–1112. doi:<https://doi.org/10.1002/2015PA002844>.
- Hoppe CJM, Flintrop CM, Rost B. 2018. The Arctic picoeukaryote *Micromonas pusilla* benefits synergistically from warming and ocean acidification. *Biogeosciences* **15**(14): 4353–4365. doi:10.5194/bg-15-4353-2018.
- Hoppe CJM, Langer G, Rost B. 2011. *Emiliana huxleyi* shows identical responses to elevated pCO₂ in TA and DIC manipulations. *Journal of Experimental Marine Biology and Ecology* **406**(1-2): 54–62. doi:10.1016/j.jembe.2011.06.008.
- Hovmöller E. 1949. The Trough-and-Ridge diagram. *Tellus* **1**(2): 62–66. doi:<https://doi.org/10.1111/j.2153-3490.1949.tb01260.x>.
- Ihnken S, Roberts S, Beardall J. 2011. Differential responses of growth and photosynthesis in the marine diatom *Chaetoceros muelleri* to CO₂ and light availability. *Phycologia* **50**(2): 182–193. doi:10.2216/10-11.1.
- Kim H, Spivack AJ, Menden-Deuer S. 2013. pH alters the swimming behaviors of the raphidophyte *Heterosigma akashiwo*: Implications for bloom formation in an acidified ocean. *Harmful Algae* **26**: 1–11. doi:<https://doi.org/10.1016/j.hal.2013.03.004>.
- Kottmeier DM, Rokitta SD, Rost B. 2016. Acidification, not carbonation, is the major regulator of carbon fluxes in the coccolithophore *Emiliana huxleyi*. *New Phytologist* **211**: 126–137. doi:10.1111/nph.13885.
- Kranz SA, Dieter S, Richter KU, Rost B. 2009. Carbon acquisition by *Trichodesmium*: the effect of pCO₂ and diurnal changes. *Limnology and Oceanography* **54**(2): 548–559. doi:10.4319/lo.2009.54.2.0548.
- Krug S, Schulz K, Riebesell U. 2011. Effects of changes in carbonate chemistry speciation on *Coccolithus braarudii*: a discussion of coccolithophorid sensitivities. *Biogeosciences* **8**: 771–777. doi:10.5194/bg-8-771-2011.
- Langer G, Geisen M, Baumann KH, Kläs J, Riebesell U, Thoms S, Young JR. 2006. Species-specific responses of calcifying algae to changing seawater carbonate chemistry. *Geochemistry, Geophysics, Geosystems* **7**(9). doi:10.1029/2005GC001227.
- Langer G, Nehrke G, Probert I, Ly J, Ziveri P. 2009. Strain-specific responses of *Emiliana huxleyi* to changing seawater carbonate chemistry. *Biogeosciences* **6**(11): 2637–2646. doi:10.5194/bg-6-2637-2009.

Li F, Fan J, Hu L, Beardall J, Xu J. 2019. Physiological and biochemical responses of *Thalassiosira weissflogii* (diatom) to seawater acidification and alkalization. *ICES Journal of Marine Science* **76**(6): 1850–1859. doi: 10.1093/icesjms/fsz028.

Müller MN, Trull TW, Hallegraeff GM. 2015. Differing responses of three Southern Ocean *Emiliania huxleyi* ecotypes to changing seawater carbonate chemistry. *Marine Ecology Progress Series* **531**: 81–90. doi: 10.3354/meps11309.

O'Brien CJ. 2015. *Global-scale distributions of marine haptophyte phytoplankton*. Phd thesis, ETH Zurich. doi: 10.3929/ethz-a-010513482.

O'Brien CJ, Vogt M, Gruber N. 2016. Global coccolithophore diversity: Drivers and future change. *Progress in Oceanography* **140**: 27–42. doi:<https://doi.org/10.1016/j.pocean.2015.10.003>.

Pančić M, Hansen PJ, Tammilehto A, Lundholm N. 2015. Resilience to temperature and pH changes in a future climate change scenario in six strains of the polar diatom *Fragilariaopsis cylindrus*. *Biogeosciences* **12**(14): 4235–4244. doi:10.5194/bg-12-4235-2015.

Riebesell U, Zondervan I, Rost B, Tortell PD, Zeebe RE, Morel FMM. 2000. Reduced calcification of marine plankton in response to increased atmospheric CO₂. *Nature* **407**(6802): 364. doi:10.1038/35030078.

Sett S, Bach LT, Schulz KG, Koch-Klavsen S, Lebrato M, Riebesell U. 2014. Temperature modulates coccolithophorid sensitivity of growth, photosynthesis and calcification to increasing seawater pCO₂. *PLoS One* **9**(2): e88308. doi:10.1371/journal.pone.0088308.

Sugie K, Yoshimura T. 2013. Effects of pCO₂ and iron on the elemental composition and cell geometry of the marine diatom *Pseudo-nitzschia pseudodelicatissima* (Bacillariophyceae). *Journal of Phycology* **49**(3): 475–488. doi:<https://doi.org/10.1111/jpy.12054>.

Sugie K, Yoshimura T. 2016. Effects of high CO₂ levels on the ecophysiology of the diatom *Thalassiosira weissflogii* differ depending on the iron nutritional status. *ICES Journal of Marine Science* **73**(3): 680–692. doi:10.1093/icesjms/fsv259.

Tatters AO, Roleda MY, Schnetzer A, Fu F, Hurd CL, Boyd PW, Caron DA, Lie AAY, Hoffmann LJ, Hutchins DA. 2013. Short- and long-term conditioning of a temperate marine diatom community to acidification and warming. *Philosophical Transactions of the Royal Society B: Biological Sciences* **368**(1627): 20120437. doi: 10.1098/rstb.2012.0437.

Trimborn S, Brenneis T, Sweet E, Rost B. 2013. Sensitivity of Antarctic phytoplankton species to ocean acidification: Growth, carbon acquisition, and species interaction. *Limnology and Oceanography* **58**(3): 997–1007. doi:10.4319/lo.2013.58.3.0997.

Wolf KKE, Hoppe CJM, Rost B. 2018. Resilience by diversity: Large intraspecific differences in climate change responses of an Arctic diatom. *Limnology and Oceanography* **63**(1): 397–411. doi:10.1002/lno.10639.